Valine 114 replacements in archaeal elongation factor 1 alpha enhanced its ability to interact with aminoacyl-tRNA and kirromycin.

ARTICLE *in* BIOCHEMISTRY · JANUARY 2003

Impact Factor: 3.02 · Source: PubMed

7 AUTHORS, INCLUDING:

Mariorosario Masullo
Parthenope University of Naples
97 PUBLICATIONS **968** CITATIONS
SEE PROFILE

Antonio Fiengo
Università degli Studi del Sannio
9 PUBLICATIONS **98** CITATIONS
SEE PROFILE

Luigi Vitagliano
Italian National Research Council
152 PUBLICATIONS **2,955** CITATIONS
SEE PROFILE

Paolo Arcari
University of Naples Federico II
112 PUBLICATIONS **1,414** CITATIONS
SEE PROFILE

Valine 114 Replacements in Archaeal Elongation Factor 1α Enhanced Its Ability To Interact with Aminoacyl-tRNA and Kirromycin†

Mariorosario Masullo,‡,§ Piergiuseppe Cantiello,§ Barbara de Paola,§ Antonio Fiengo,§ Luigi Vitagliano,|| Adriana Zagari,||,⊥,@ and Paolo Arcari*,§,⊥

Dipartimento di Scienze Farmacobiologiche, Università di Catanzaro Magna Graecia, Roccelletta di Borgia, I-88021 Catanzaro, Italy, Dipartimento di Biochimica e Biotecnologie Mediche, Università di Napoli Federico II, and CEINGE Biotecnologie Avanzate Scarl, via S. Pansini 5, I-80131 Napoli, Italy, and Istituto di Biostrutture e Bioimmagini, CNR, and Dipartimento di Chimica Biologica, Sezione Biostrutture, Via Mezzocannone 6, I-80134 Napoli, Italy

Received July 10, 2002; Revised Manuscript Received September 16, 2002

ABSTRACT: Valine 114 in the D^{109}AAILVVA sequence of elongation factor 1α from the archaeon *Sulfolobus solfataricus* (*Ss*EF-1α) was substituted with an acidic (V114E), basic (V114K), or cavity-forming (V114A) residue, and the effects on the biochemical properties of the factor were investigated. This sequence is well-conserved among most of eukaryal and eubacterial counterparts, and in the three-dimensional structure of *Ss*EF-1α, V114 is located in a hydrophobic pocket near the first GDP-binding consensus sequence G_{13}XXXXGK[T,S] [Vitagliano, L., Masullo, M., Sica, F., Zagari, A., and Bocchini, V. (2001) *EMBO J. 20*, 5305−5311]. These mutants displayed functions absent in the wild-type factor. In fact, although they exhibited a rate in poly(Phe) incorporation almost identical to that of *Ss*EF-1α, V114K and V114A exhibited an affinity for GDP and GTP higher and a capability to bind heterologous aa-tRNA stronger than that elicited by *Ss*EF-1α but similar to that of eubacterial EF-Tu. V114E instead displayed not only a weaker binding capability for aa-tRNA but also a lower affinity for GDP. The intrinsic GTPase activity of V114E was drastically reduced compared to those of *Ss*EF-1α, V114K, and V114A. Interestingly, the decreased intrinsic GTPase activity of V114E was partially restored by kirromycin, an effect already observed for the G13A mutant of *Ss*EF-1α [Masullo, M., Cantiello, P., de Paola, B., Catanzano, F., Arcari, P., and Bocchini, V. (2002) *Biochemistry 41*, 628−633]. Finally, the V114A substitution showed only a marginal effect on both the thermostability and thermophilicity of *Ss*EF-1α, whereas V114K and V114E replacements strongly destabilized the molecule.

Eukaryal and archaebacterial elongation factor 1α and its eubacterial counterpart EF-Tu[1] play a fundamental role in the elongation cycle of protein biosynthesis. In fact, these enzymes catalyze the delivery of aminoacylated tRNA (aa-tRNA) to the elongating peptide on the ribosome (*1*). EF-1α from the hyperthermophilic archaeon *Sulfolobus solfataricus* (*Ss*EF-1α) is a monomeric protein of 435 amino acid residues (*2*) and belongs to the class of GTP binding proteins (*3*). It possesses an intrinsic GTPase activity revealed in the presence of a molar concentration of NaCl ($GTPase^{Na}$) (*4*) and possesses a high thermophilicity and thermostability (*5*). The crystal structure of *Ss*EF-1α in complex with GDP has recently been determined by X-ray crystallography at 1.8 Å resolution (*6*). As found for eubacterial EF-Tu (*7*−*9*) and eukaryal EF-1α (*10*), three structurally distinct domains have been identified. The N-terminal domain, which contains the nucleotide binding site, presents an α/*β* structure with a six-stranded *β*-sheet surrounded by seven α-helices. The other two domains display a *β*-barrel structure.

In contrast to EF-Tu, which has been thoroughly studied by site-directed mutagenesis, only limited information has been derived for eukaryal and archaeabacterial EF-1α by analyzing the effects produced by specific amino acid substitutions. Indeed, mutational studies on eukaryal EF-1α have been carried out only on the N_{153}KMD guanine binding motif of yeast EF-1α (*11*). In the framework of our ongoing research on *Ss*EF-1α mutants, we have recently analyzed the functional role of Gly13 in the first GDP binding sequence motif of *Ss*EF-1α (residues 12−19) (*3*). The overall results suggested that the G13A substitution affected mainly the biochemical properties of the enzyme, whereas its thermostability remained practically unaltered (*12*). With the aim of elucidating the role played by amino acid side chains in this region, we extended our analysis to the residue that in the three-dimensional (3D) structure of *Ss*EF-1α faces Gly13. This residue, Val114 (Val104 in EcEF-Tu), is a rather

† This work was supported by CNR, PRIN 2001 (Rome), and the European Community Biotechnology Program (Contract BIO4-CT97-2188).

* To whom correspondence should be addressed. Telephone: +39 081.7463120. Fax: +39 081.7463653. E-mail: arcari@dbbm.unina.it.

‡ Università di Catanzaro Magna Graecia.

§ Università di Napoli Federico II.

|| CNR.

⊥ CEINGE Biotecnologie Avanzate Scarl.

@ Sezione Biostrutture.

[1] Abbreviations: EF, elongation factor; *Ss*, *Sulfolobus solfataricus*; *Ec*, *Escherichia coli*; V114A, V114E, and V114K, *Ss*EF-1α carrying the corresponding amino acid substitution; $GTPase^{Na}$, intrinsic GTPase of *Ss*EF-1α triggered by 3.6 M NaCl; CD, circular dichroism.

10.1021/bi026428n CCC: $22.00
Published on Web 11/15/2002

well conserved amino acid residue among EF-1α and EF-Tu sequences (*13*). Although it does not belong to the nucleotide binding site, it was chosen as a mutagenic target to study the role of this semiinvariant position on the functional and structural properties of *Ss*EF-1α. In addition, in the 3D structure of *Ss*EF-1α (*6*), Val114 is close to the P-loop, an invariant structural element occurring in all EF-1α and EF-Tu species. The biochemical and biophysical characterization of the V114K, V114E, and V114A mutants of *Ss*EF-1α indicated that these mutations affected some of the properties of the factor. Interestingly, some of these mutated forms are endowed with functions absent in the wild-type enzyme. Finally, the structural and functional alterations caused by Val114 substitution have been analyzed on the basis of the recently determined 3D structure of *Ss*EF-1α (*6*).

MATERIALS AND METHODS

Chemicals, Enzymes, and Buffers. Restriction enzymes, modifying enzymes, labeled compounds, and chemicals were as reported previously (*14*); plasmid DNA, genomic DNA, and labeled probes were prepared as described previously (*15*). The following buffers were used: buffer A [20 mM Tris-HCl (pH 7.8), 50 mM KCl, and 10 mM $MgCl_2$] and buffer B [20 mM Tris-HCl (pH 7.8), 10 mM $MgCl_2$, and 1 mM DTT].

Plasmid Construction, Expression, and Purification of the Mutant Elongation Factors. The expression vector used as a template was a pT7-7 derivative, containing the gene encoding elongation factor 1α from *S. solfataricus* (*14*). We have used six self-complementary primers (G_{328}CTGCAATT-CTAAAAGTTTCTGC, G_{328}CTGCAATTCTAGAAGTTTC-TGC, and G_{328}CTGCAATTCTAGCAGTTTCTGC), introducing the $G_{340}T \rightarrow AA$, $T_{341} \rightarrow A$, and $T_{341} \rightarrow C$ base substitutions, respectively, as numbered from the *Ss*EF-1α starting codon. This allowed the synthesis of new plasmids carrying the V114K, V114E, and V114A mutations in the elongation factor. These plasmids were obtained by following to the Stratagene mutagenesis kit procedure. The product of each PCR was then used to transform XL11 epicurian competent cells; recombinant clones were selected for identification of those containing the desired mutations. The selected clones were then used to transform *Escherichia coli* BL21(DE3) cells (*16*) which were then grown overnight at 37 °C in 10 mL of L-broth containing 100 μg/mL ampicillin. The culture was then diluted 1:100 in a final volume of 1 L and grown to an absorbance of 0.7 at 600 nm. Induction (3 h) was performed by adding isopropyl β-D-thiogalactopyranoside up to a final concentration of 0.4 mM. The bacterial cells were collected by centrifugation, resuspended in buffer A (6 mL/g of wet cells) containing 15% glycerol and 1 mM phenylmethanesulfonyl fluoride, and disrupted by a system of cell disruption at 2 kbar (Constant System, Ltd.). The V114K, V114E, and V114A mutant elongation factors were purified according to the procedure already reported for wild-type recombinant *Ss*EF-1α (*14*), dialyzed against buffer A containing 50% (v/v) glycerol, and stored at −20 °C.

SsEF-1α Mutant Assays and Characterization. Isolation of total tRNA and ribosome from *S. solfataricus* was performed as described previously (*17*). Poly(U)-directed poly(Phe) synthesis and the determination of the concentration of *Ss*EF-1α and its mutated forms to obtain half of its maximum activity (K_{act}) were carried out as reported previously (*12*).

The preparation of Phe-*Ec*tRNA^{Phe}, the formation of the *Ss*EF-1α·[γ-^{32}P]GTP·Phe-*Ec*tRNA^{Phe} ternary complex, and the protection against spontaneous deacylation of [^{3}H]Phe-*Ec*tRNA^{Phe} were carried out as described previously (*18*, *19*).

The ability of the V114K, V114E, and V114A mutants to form a binary complex with [^{3}H]GDP was assayed as described previously (*20*). The number of [^{3}H]GDP binding sites and the apparent equilibrium dissociation constant (K'_d) of the complex between the mutated forms of *Ss*EF-1α and [^{3}H]GDP were determined with a Scatchard plot in the presence of 0.5 μM V114K, 0.5 μM V114A, or 1 μM V114E and 0−100 μM [^{3}H]GDP (specific activity of 500−950 cpm/pmol). The K'_d for GTP was determined by competitive binding experiments in the presence of 25 μM [^{3}H]GDP (specific activity of 500 cpm/pmol) at different GTP concentrations. The apparent dissociation rate constants for the V114K·GDP, V114E·GDP, and V114A·GDP complexes were determined as reported previously (*20*).

The GTPase^{Na} activity was measured in the presence of 3.6 M NaCl (*4*). Unless otherwise indicated, the reaction mixture contained 0.5−1 μM purified factor and 50 μM [γ-^{32}P]GTP (specific activity of 200−300 cpm/pmol) in 200 μL of buffer B. The reaction was followed kinetically up to 30 min at 60 °C, and 40 μL aliquots were analyzed for the amount of $^{32}P_i$ released. The k_{cat} of GTPase^{Na}, the K_m for [γ-^{32}P]GTP, and the GDP inhibition constants were determined as reported previously (*17*). Commercial GTP and [γ-^{32}P]GTP were incubated for 20 min at 25 °C in buffer B containing 1 mM DTT, in the presence of 50−500 μM phosphoenolpyruvate and 4−40 μg of pyruvate kinase to convert the GDP traces in GTP.

The effect of kirromycin on the intrinsic GTPase activity of the mutated factors was tested as previously described (*12*) in the presence of 50 μM antibiotic and 0.3 μM protein in the case of V114K and V114A or 3 μM protein in the case of V114E; moreover, the effect of kirromycin on V114E was tested in the range of 0−60 μM antibiotic.

Thermophilicity and Heat Stability of SsEF-1α and Its V114K, V114E, and V114A Mutants. The thermophilicity of the V114K, V114E, and V114A mutants was checked by measuring the amount of GTPase^{Na} in the temperature range of 40−95 °C. At each temperature, the reaction was carried out in the presence of 0.5 μM V114K, 0.5 μM V114E, or 1 μM V114A and 50 μM [γ-^{32}P]GTP (specific activity of 300 cpm/pmol), and was followed kinetically; at time intervals depending on temperature, 40 μL aliquots were withdrawn and analyzed for the amount of $^{32}P_i$ released (*4*). The data were treated according to the Arrhenius equation, and the energetic parameters of activation were calculated as reported previously (*21*).

Heat inactivation of the V114K, V114E, and V114A mutants was evaluated by incubating 5 μM protein in buffer A for 10 min at selected temperatures in the interval of 70−99 °C. After heat treatment, 40 μL aliquots were cooled on ice for 30 min and then analyzed for their [^{3}H]GDP binding and their residual GTPase^{Na} activity. GDP binding reaction mixtures contained 1 μM mutated factors and 50 μM [^{3}H]-GDP (specific activity of 700 cpm/pmol) in a final volume of 50 μL. The aliquots were incubated for 30 min at 60 °C

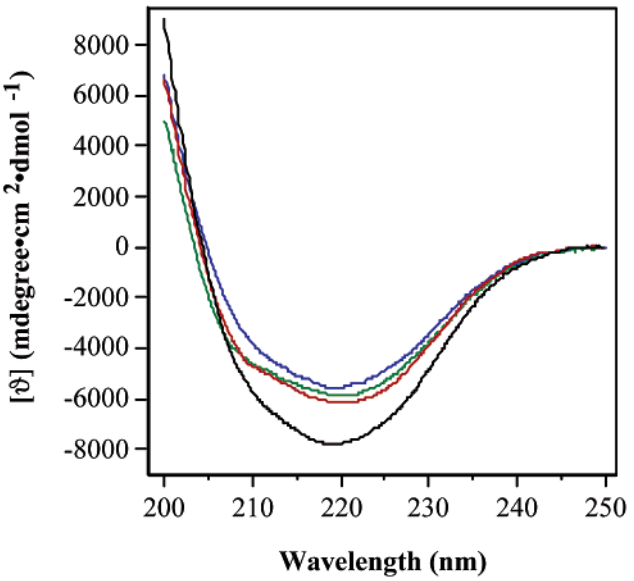

FIGURE 1: Far-UV CD spectra of *Ss*EF-1α and its mutated forms. Measurements were recorded at 25 °C at a protein concentration of 0.1 mg/mL in 10 mM Tris-HCl buffer (pH 7.5): *Ss*EF-1α (green), V114K (blue), V114A (red), and V114E (black).

and then analyzed as described above. GTPase^{Na} reaction mixtures contained 0.5 μM mutated factors and 50 μM [γ-^{32}P]GTP (specific activity of 300 cpm/pmol) in a final volume of 50 μL. The mixtures were incubated for 30 min at 60 °C and then analyzed for the amount of $^{32}P_i$ released, as described above. UV melting curves were obtained in the temperature range of 60−100 °C as reported previously (*18*). CD measurements were performed with a JASCO J-710 spectropolarimeter, calibrated with an aqueous solution of *d*-10-(+)-camphorsulfonic acid at 290 nm. Far-UV CD spectra were recorded using a 0.1 cm cuvette at a time constant of 4 s and 2 nm bandwidth.

Molecular Graphics Analyses. The structural alterations caused by the mutations were analyzed using as a template the structure of *Ss*EF-1α in complex with GDP (PDB entry 1JNY) refined at 1.8 Å resolution (*6*). The crystal form used for this crystallographic study contains two similar independent molecules in the asymmetric unit. Molecule A, which displays better defined electron densities, was used in the structural analysis presented here, carried out using the program O (*22*). The programs MOLSCRIPT (*23*) and Raster3D (*24*) were used to generate Figure 9.

RESULTS

Molecular Properties of Mutated SsEF-1α. Purified *Ss*EF-1α mutants showed, under either native (gel filtration) or denaturing (SDS−PAGE) conditions, M_r values identical to that of *Ss*EF-1α. Moreover, *Ss*EF-1α and its V114K, V114E, and V114A mutants were analyzed by CD at 25 °C. All the CD spectra reported in Figure 1 exhibited a minimum around 220 nm. The results suggested that V114A and V114K possessed an extent of secondary structure comparable to that exhibited by *Ss*EF-1α, whereas the more negative molar ellipticity at 220 nm of V114E may indicate an increased level of secondary structure.

Biochemical Properties of V114A, V114E, and V114K. The rate of poly[^{3}H]Phe synthesis catalyzed by the V114K, V114E, and V114A mutants was almost identical to that

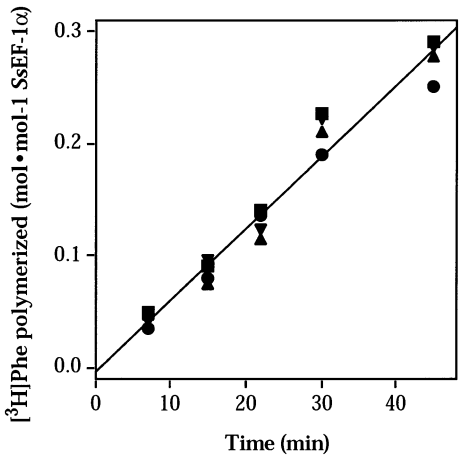

FIGURE 2: Poly(U)-directed poly(Phe) synthesis promoted by *Ss*EF-1α and its mutated forms. Three hundred microliters of the reaction mixture contained 25 mM Tris-HCl (pH 7.5), 19 mM magnesium acetate, 10 mM NH_4Cl, 10 mM dithiothreitol, 2.4 mM ATP, 1.6 mM GTP, 0.16 mg/mL poly(U), 3 mM spermine, 0.25 μM *Ss* ribosome, 80 μg/mL *Ss*tRNA, and 2.4 μM [^{3}H]Phe (specific activity of 5413 cpm/pmol). The reaction was started by addition of a final concentration of 0.5 μM *Ss*EF-1α (▼), V114K (▲), V114A (●), and V114E (■). The reaction was carried out at 60 °C, and at the indicated times, 50 μL aliquots were withdrawn, chilled on ice, and then analyzed for the amount of [^{3}H]Phe polymerized. The curve shows the behavior of all the reported experimental points.

Table 1: Kinetic Parameters of Poly(Phe) Synthesis Promoted by *Ss*EF-1α and Its Mutated Forms[a]

	K_{act} (μM)	V (pmol min^{-1})		K_{act} (μM)	V (pmol min^{-1})
*Ss*EF-1α	0.09	0.38	V114E	0.11	0.40
V114K	0.06	0.36	V114A	0.04	0.36

[a] One hundred microliters of the reaction mixture, prepared as described in the legend of Figure 2, contained each elongation factor (0.05−4 μM). The reaction was allowed to proceed for 25 min at 60 °C and then the mixture analyzed for the amount of [^{3}H]Phe that was polymerized. The rate of [^{3}H]Phe polymerization was calculated, and K_{act} and V were derived from Lineweaver−Burk plots of the data.

displayed by *Ss*EF-1α (Figure 2). However, the concentrations of V114A and V114K required to obtain half of its maximum activity (K_{act}) were ~2.3- and ~1.5-fold lower, respectively, than that required by *Ss*EF-1α, whereas in the case of V114E, the value was ~1.2-fold higher (Table 1).

The ability of *Ss*EF-1α mutants to interact with aa-tRNA was assayed by measuring the amount of ternary complex formation as evaluated by gel filtration (*18*). Compared to *Ss*EF-1α, V114E was unable to bind heterologous Phe-*Ec*tRNA^{Phe} and [γ-^{32}P]GTP, whereas in the case of V114K and V114A, the formation of a ternary complex was comparable to that exhibited by *Ec*EF-Tu used as control (Figure 3). It has to be noted that in the absence of Phe-*Ec*tRNA^{Phe} no [γ-^{32}P]GTP was bound to *Ss*EF-1α and its V114 mutants. The interaction between *Ss*EF-1α or its mutated forms and aa-tRNA was also analyzed by evaluating the protection exerted by these elongation factors in complex with GDP or GppNHp from the spontaneous deacylation of [^{3}H]Phe-*Ec*tRNA^{Phe} (Figure 4). The results that were obtained showed that *Ss*EF-1α, V114K, and V114A in complex with GppNHp exerted protection against spontaneous deacylation, whereas V114E was almost unefficient. In addition, as already reported for *Ss*EF-1α (*19*), the mutated forms

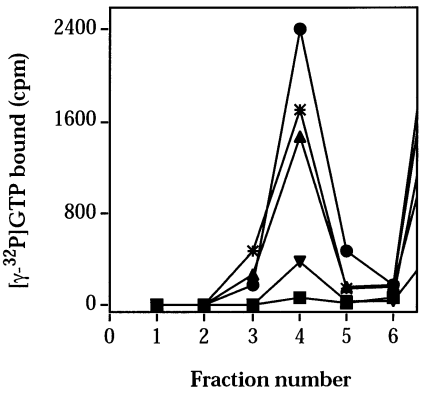

FIGURE 3: Interaction of Phe-*Ec*tRNA^{Phe} with *Ss*EF-1α, its mutated forms, or *Ec*EF-Tu. Thirty-five microliters of buffer A contained 60 mM NH_4Cl, 0.2 μM *Ss*EF-1α (▼), *Ec*EF-Tu (∗), V114K (▲), V114A (●) or V114E (■), 1 μM Phe-*Ec*tRNA^{Phe}, 1 μM [γ-^{32}P]-GTP (specific activity of 8300 cpm/pmol), 1 mM phosphoenolpyruvate, and 40 μg/mL pyruvate kinase. The reaction mixture was incubated for 10 min at 0 °C, and then 30 μL was loaded onto a Sephadex G-25 column (0.4 cm × 15 cm) equilibrated with buffer A. Fractions (100 μL) were collected and counted for radioactivity. Blanks run in the absence of Phe-*Ec*tRNA^{Phe} were subtracted.

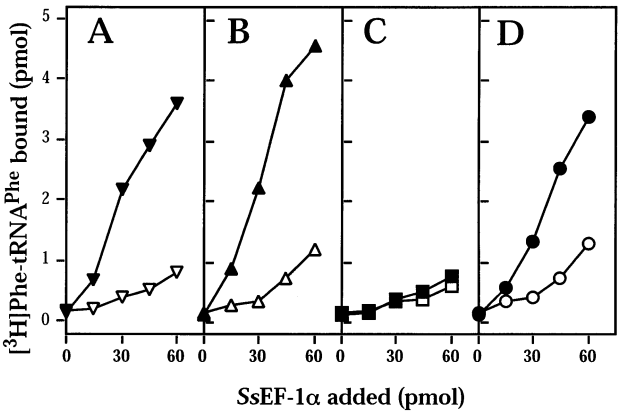

FIGURE 4: Protection against the spontaneous deacylation of [^{3}H]-Phe-*Ec*tRNA^{Phe} by *Ss*EF-1α and its mutated forms. Thirty microliters of the reaction mixture containing 25 mM Tris-HCl buffer (pH 7.8), 10 mM NH_4Cl, 10 mM DTT, 20 mM magnesium acetate, and 5.3 pmol of [^{3}H]Phe-*Ec*tRNA^{Phe} (specific activity of 2065 cpm/pmol) was preincubated for 1 h at 0 °C to allow ternary complex formation in the presence of the indicated amount of *Ss*EF-1α (A), V114K (B), V114E (C), or V114A (D) in complex with GDP (empty symbols) or GppNHp (filled symbols). The deacylation reaction was carried out for 1 h at 50 °C, and the residual amount of [^{3}H]Phe-*Ec*tRNA^{Phe} was determined as reported in Materials and Methods.

Table 2: Affinity of *Ss*EF-1α and Its Mutated Forms for Guanine Nucleotides

	K'_d (μM)			
	GDP	GTP	k_{-1} (GDP) (min^{-1})	k_{+1} (GDP) (μM^{-1} min^{-1})
*Ss*EF-1α	1.6	35	0.12	0.08
V114K	0.5	4	0.28	0.56
V114E	137.0	–	–	–
V114A	1.0	25	–	–

analyzed in this work displyed a protection capability even when complexed with GDP but with a lower efficiency.

As reported in Table 2, the affinity of *Ss*EF-1α mutants for GDP and GTP was slightly higher than that of wild-type *Ss*EF-1α in the case of V114K and V114A, whereas in the case of V114E, it was ∼2 orders of magnitude lower.

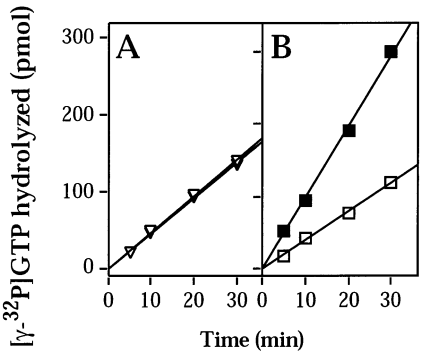

FIGURE 5: Effect of kirromycin on the GTPase^{Na} of *Ss*EF-1α and V114E. Two hundred thirty microliters of the reaction mixture contained 0.3 μM *Ss*EF-1α (A) or 3 μM V114E (B); the reaction was carried out either in the absence (empty symbols) or in the presence (filled symbols) of 50 μM kirromycin, in buffer B containing 3.6 M NaCl and 50 μM [γ-^{32}P]GTP (specific activity of 300 cpm/pmol). This reaction was carried out at 60 °C, and at the indicated times, 50 μL aliquots were withdrawn and analyzed for the amount of $^{32}P_i$ released.

Table 3: Intrinsic GTPase Activity of *Ss*EF-1α and Its Mutated Forms

	K_m (μM)	k_{cat} (min^{-1})	k_{cat}/K_m (min^{-1} μM^{-1})	K_i (GDP) (μM)
*Ss*EF-1α	2.7	0.80	0.296	0.8
V114K	6.1	0.30	0.049	1.9
V114E	31.0	0.02	0.001	–
V114A	2.6	0.30	0.115	1.0

V114E Showed a GTPase^{Na} that Was Stimulated by Kirromycin. *Ss*EF-1α displays a very low intrinsic GTPase activity that was highly enhanced in the presence of NaCl at molar concentrations (*4*). The rate of turnover of GTPase^{Na} elicited by V114K and V114A mutants was comparable to that of *Ss*EF-1α (not shown), whereas the hydrolytic rate of V114E was significantly lower than that of *Ss*EF-1α (Figure 5A). At 60 °C, the affinity for GTP (Table 3) decreased by 2.3- and 11.5-fold in the case of V114K and V114E, respectively, and it was identical to that of *Ss*EF-1α in the case of V114A. The k_{cat} of the reaction was 2.7-fold lower for both V114K and V114A and 40-fold lower for V114E. As a consequence, the catalytic efficiency of the GTPase^{Na} of V114E was 2 orders of magnitude lower than that of *Ss*EF-1α (Table 3). As already reported for *Ss*EF-1α (*4*), the GTPase^{Na} of the *Ss*EF-1α mutants was competitively inhibited by GDP with a grade of efficiency comparable to that of *Ss*EF-1α.

Kirromycin did not stimulate the GTPase^{Na} of *Ss*EF-1α (Figure 5A). Vice versa, kirromycin enhanced the rate of GTP hydrolysis catalyzed by V114E (Figure 5B) but not that of the other two mutants (not shown). The maximum stimulatory effect was observed around 40 μM kirromycin (Figure 6A), and the concentration of the antibiotic required for half of its maximum activation was calculated to be 2 μM **(**Figure 6B).

Thermostability of SsEF-1α and Its Mutated Forms. The heat inactivation was tested by assaying the residual [^{3}H]-GDP binding ability of *Ss*EF-1α mutants and compared to that of the wild-type factor. As reported in Figure 7A, *Ss*EF-1α was half-inactivated after exposure for 10 min at 94 °C, whereas V114K, V114E, and V114A exhibited lower half-inactivation temperatures of 79, 86, and 92 °C, respectively. Similar results were obtained using the GTPase^{Na} as a tool

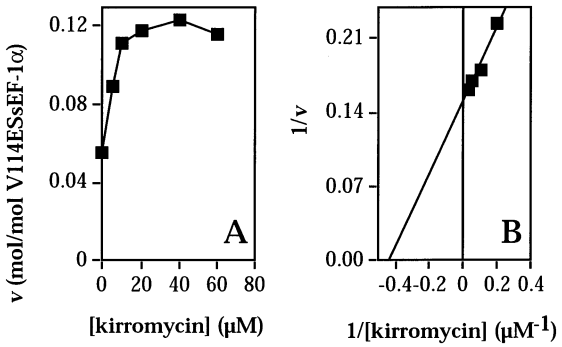

FIGURE 6: Affinity of V114E for kirromycin in the GTPase^{Na}. (A) The reaction mixture contained 3 μM V114E and was prepared as described in Materials and Methods, in the presence of kirromycin at the indicated concentration. The reaction was followed kinetically at 60 °C, and the slope of the linear part of each kinetic trace was plotted as a function of the kirromycin concentration. (B) The data reported in panel A were treated with the Lineweaver−Burk equation, after subtraction of the GTPase^{Na} activity of V114E in the absence of kirromycin.

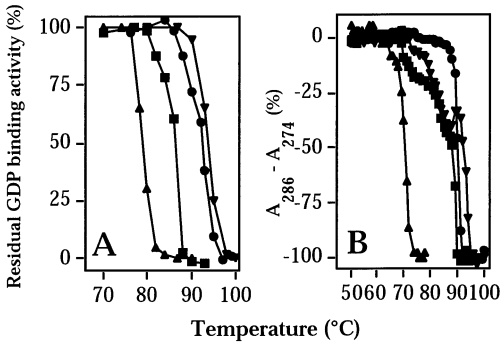

FIGURE 7: Heat stability of *Ss*EF-1α and its mutated forms. Residual [^{3}H]GDP binding ability (A) and UV melting curves (B) of *Ss*EF-1α (▼), V114K (▲), V114A (●), and V114E (■). For other details, see Materials and Methods.

to investigate the heat inactivation. The heat stability of *Ss*EF-1α and its mutants was also examined by ultraviolet-monitored thermal denaturation (Figure 7B). The temperatures for half-denaturation were close to that determined from the inactivation profile (Figure 7A). In fact, compared to that of *Ss*EF-1α (92 °C), these temperatures were 22, 4, and 2 °C lower for V114K, V114E, and V114A, respectively. The heat denaturation was also assessed by measuring the loss of secondary structure by CD measurements. The temperatures for half-denaturation that were observed were comparable to those obtained from UV melting profiles (not shown).

The thermophilicities of V114K, V114E, and V114A were compared to that of *Ss*EF-1α, evaluating the GTPase^{Na} at increasing temperatures. V114A exhibited the highest activity at 90 °C, a temperature identical to that measured for *Ss*EF-1α, whereas V114E and V114K exhibited the highest activity at 65 and 80 °C, respectively, after inactivation had occurred (Figure 8A). The analysis of the rising part of the curves according to the Arrhenius equation (Figure 8B) allowed the calculation of the energetic parameters of activation of the GTPase^{Na} of *Ss*EF-1α and its mutated forms. Both the energy and entropy of activation for V114K, V114E, and V114A were lower than those of *Ss*EF-1α (Table 4).

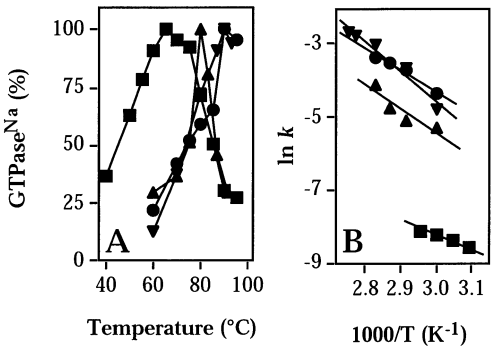

FIGURE 8: Thermophilicity of *Ss*EF-1α and its mutated forms. The GTPase^{Na} activity was assayed as described in the legend of Figure 5 at the indicated temperatures (A) and reported as the number of moles of [γ-^{32}P]GTP hydrolyzed per minute per mole of protein for *Ss*EF-1α (▼), V114K (▲), V114A (●), and V114E (■). (B) Arrhenius analysis of the data in the range of 40−60 °C for V114E, 60−80 °C for V114K, and 60−87 °C for V114A and *Ss*EF-1α.

Table 4: Energetic Parameters of the GTPase^{Na} of *Ss*EF-1α and Its Mutated Forms[a]

	E (kJ mol^{-1})	ΔS^* (J mol^{-1} K^{-1})	ΔG^* (kJ mol^{-1})
*Ss*EF-1α	69	−87	95
V114K	55	−135	97
V114E	36	−214	105
V114A	50	−140	94

[a] The values of *E* were derived from the data reported in Figure 7B. ΔS^* and ΔG^* were calculated at 60 °C.

DISCUSSION

In *Ss*EF-1α, valine 114 (Val104 in *Ec*EF-Tu) belongs to the D^{109}AAILVVA conserved sequence fragment of EF-1α and EF-Tu enzymes (*13*, *25*). The 3D structures of *Ss*EF-1α (*6*) and *Ec*EF-Tu (*7*) indicate that this residue is located in a structurally conserved β-strand (strand B4) belonging to the β-sheet core of the GDP-binding domain of these proteins. It is worth mentioning that strand B4 is flanked by α-helices A (amino acids 19−30) and C (amino acids 131−142). The Val114 side chain is located in a hydrophobic pocket lined by the side chains of Val11, Lys19, Leu22, and Ile112 (Figure 9). Therefore, the proximity of the Val114 side chain to the amino acids involved in the binding of the phosphate moiety of GDP/GTP (P-loop) makes this residue interesting for mutational studies. Site-directed mutagenesis in this region was never undertaken on both EF-1α and EF-Tu. The hydrophobic side chain of Val114 (Figure 9) was therefore replaced with a negatively (glutamic acid) and positively (lysine) charged side chain. In addition, the effects produced by the cavity-forming V114A mutation were also analyzed.

All three mutations did not significantly affect the requirement of *Ss*EF-1α in poly(U)-directed poly(Phe) incorporation because they exhibited almost identical reaction rates (Figure 2). The only differences involved the K_{act} values of the V114A and V114K mutants that were lower compared to that of wild-type *Ss*EF-1α (Table 1). These differences could be ascribed to an improved capability of these two mutants to bind aa-tRNA and GTP with respect to *Ss*EF-1α (Figure 3). This behavior was also evaluated by analyzing the capability of *Ss*EF-1α and its mutated forms to protect aa-tRNA from spontaneous deacylation (Figure 4). The results obtained confirmed the behavior of V114E, whereas in the

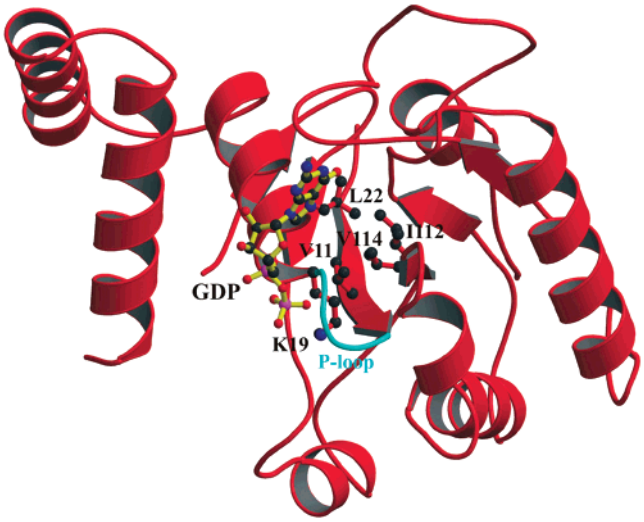

FIGURE 9: Location of Val114 in the 3D structure of *Ss*EF-1α complexed with GDP. For clarity, only the GDP-binding domain (residues 4−228) is shown. Residues 66−76 are missing as they are disordered in the crystal structure.

case of V114K and V114A, the extent of protection was almost similar to that found for *Ss*EF-1α. The differences observed between the results reported in Figures 3 and 4 could be due to the lower affinity of the elongation factors for GppNHp with respect to that elicited for GTP (*17*, *26*). From a structural point of view, the distance (>20 Å) from the mutated position to the aa-tRNA binding site in *Tt*EF-Tu·GppNHp·Phe-tRNA^{Phe} and *Tt*EF-Tu·GppNHp·Cys-tRNA^{Cys} complexes (*27*, *28*) suggested either specific long-range effects or differences between the aa-tRNA binding site of *Ss*EF-1α and that of *Tt*EF-Tu.

As far as the binding to guanine nucleotides is concerned, it is worth noting that the V114A and V114K mutants also exhibited slightly higher affinities for GTP and GDP. In the case of V114K, the increase in the affinity for GDP was due to the association rate constant being higher than the dissociation rate constant (Table 2). V114E, which instead displayed a very low affinity for GDP, showed an affinity for Phe-*Ec*tRNA^{Phe} even lower than that of wild-type *Ss*EF-1α (Figures 3 and 4C).

Contrary to the increased affinity for GTP and GDP, V114K displayed an intrinsic GTPase activity that was characterized by a lower affinity for GTP and GDP (Table 3), whereas V114A showed a GTPase^{Na} activity almost identical to that of *Ss*EF-1α. With regard to V114E, the reduced affinity for guanine nucleotides is also accompanied by a catalytic efficiency 2 orders of magnitude lower in the GTPase^{Na} activity. These data indicated that the insertion of a negatively charged side chain into the B4 strand affected both the affinity for guanine nucleotides and GTP hydrolysis. They may be thoroughly explained by considering the repulsion between the negative charges of the glutamic acid and the phosphate moiety of GDP/GTP (Figure 9). The analysis of the energetic values reported in Table 4 provides additional details about this issue. In fact, the GTPase^{Na} free energy of activation of V114E measured at 60 °C was lower than that displayed by *Ss*EF-1 α, V114A, or V114K. On the other hand, the energy of activation of this reaction was lower for V114E. Therefore, the activation state of the hydrolytic reaction catalyzed by V114E was less entropically favored with respect to the other elongation factors. Interestingly, the impairment in GDP binding, GTP hydrolysis, and ternary complex formation observed for V114E mutant was not reflected in the poly(Phe) incorporation reaction probably because this assay is more complex than the others. In fact, the possibility that the presence of other macromolecular components, mainly ribosome and aa-tRNA synthetase, could somehow abolish the effects produced by the mutation on the specific biochemical properties of *Ss*EF-1α cannot be ruled out.

As already found for the G13A mutant of *Ss*EF-1α (*12*), the GTPase^{Na} activity of V114E was partially restored by kirromycin. This antibiotic, which is a classical inhibitor of protein biosynthesis in eubacteria, does not affect the activity of wild-type *Ss*EF-1α. Such a different behavior between eubacterial EF-Tu and archaeal EF-1α toward kirromycin has been interpreted as being due to different architectures which made archaeal EF-1α different from eubacterial EF-Tu (*29*, *30*). In fact, among the eight amino acid residues that in *Ec*EF-Tu were involved in the binding of kirromycin (L120, Q124, Y160, I298, G316, Q329, A375, and E378) (*31*−*33*), only A375 is conserved in *Ss*EF-1α as A410. Recent crystallographic investigations on the complex between EF-Tu and a kirromycin-related antibiotic (aurodox) have demonstrated that the domain I−domain III interface is involved in inhibitor binding (*33*). The rather different domain I−domain III interface in EF-Tu and *Ss*EF-1α may account for the different role that kirromycin plays in these enzymes. The finding that the intrinsic GTPase activity of G13A and V114E can be enhanced by this antibiotic suggested that these mutations might indirectly alter the interactions of the domain I−domain III interface, even though they are far from this location.

With regard to the thermal properties of the three *Ss*EF-1α mutants, the V114A substitution caused only a marginal impairment of the thermostability (Figure 7) and thermophilicity (Figure 8) of *Ss*EF-1α. These findings suggested that the cavity produced by the lack of two methyl groups following the Val → Ala replacement may be filled by a local rearrangement of the protein structure. In the case of the V114E mutant, the effect on the heat stability was more pronounced for GDP binding, thus suggesting that the V114E replacement affected mostly the stability of the G-domain. On the other hand, the V114K substitution showed instead a more dramatic effect on the thermostability of the entire molecule. These effects may be ascribed to the larger size of the Lys side chain, which may produce large deformations of this closely packed region of the protein.

In conclusion, the biochemical data reported here show that the hydrophobic side chain of the semiinvariant Val114 is not essential to EF-1α activity since the V114A mutant and the wild-type enzyme displays very similar properties. On the other hand, our data demonstrate that the integrity of the pocket surrounding the B4 strand is important for *Ss*EF-1α. Indeed, the insertion of bulky and charged residues into this region produces significant alterations in *Ss*EF-1α enzymatic activity and thermostability.

ACKNOWLEDGMENT

We gratefully acknowledge Dr. Francesca Catanzano for CD measurements.

REFERENCES

1. Kaziro, Y. (1978) *Biochim. Biophys. Acta 505*, 95−127.
2. Arcari, P., Gallo, M., Ianniciello, G., Dello Russo A., and Bocchini, V. (1994) *Biochim. Biophys. Acta 1217*, 333−337.
3. Dever, T. E., Glynias, M. J., and Merrick, W. C. (1987) *Proc. Natl. Acad. Sci. U.S.A. 84*, 1814−1818.
4. Masullo, M., De Vendittis, E., and Bocchini, V. (1994) *J. Biol. Chem. 269*, 20376−20379.
5. Masullo, M., Raimo, G., and Bocchini, V. (1993) *Biochim. Biophys. Acta 1162*, 35−39.
6. Vitagliano, L., Masullo, M., Sica, F., Zagari, A., and Bocchini, V. (2001) *EMBO J. 20*, 5305−5311.
7. Kjeldgaard, M., and Nyborg, J. (1992) *J. Mol. Biol. 223*, 721−742.
8. Polekhina, G., Thirup, S., Kjeldgaard, M., Nissen, P., Lippman, C., and Nyborg, J. (1996) *Structure 4*, 1141−1151.
9. Song, H., Parson, M. R., Rowsell, S., Leonard, G., and Phillips, S. E. (1999) *J. Mol. Biol. 285*, 1245−1256.
10. Andersen, G. R., Pedersen, L., Valente, L., Chatterjee, I. I., Kinzy, T. G., Kjeldgaard, M., and Nyborg, J. (2000) *Mol. Cell 5*, 1261−1266.
11. Carr-Schmid, A., Durko, N., Cavallius, J., Merrick, W. C., and Kinzy, T. G. (1999) *J. Biol. Chem. 274*, 30297−30302.
12. Masullo, M., Cantiello, P., de Paola, B., Catanzano, F., Arcari, P., and Bocchini, V. (2002) *Biochemistry 41*, 628−633.
13. Baldauf, S. L., Palmer, J. D., and Ford Doolittle, W. (1996) *Proc. Natl. Acad. Sci. U.S.A. 93*, 7749−7754.
14. Ianniciello, G., Masullo, M., Gallo, M., Arcari, P., and Bocchini, V. (1996) *Biotechnol. Appl. Biochem. 23*, 41−45.
15. Maniatis, T., Fritsch, E. F., and Sambrook, J. (1982) *Molecular Cloning*: *A Laboratory Manual*, Cold Spring Harbor Laboratory Press, Plainview, NY.
16. Studier, F. W., Rosemberg, A. H., Dunn, J. J., and Dubendorff, J. W. (1990) *Methods Enzymol. 185*, 60−89.
17. Masullo, M., Ianniciello, G., Arcari, P., and Bocchini, V. (1997) *Eur. J. Biochem. 243*, 468−473.
18. Arcari, P., Masullo, M., Arcucci, A., Ianniciello, G., de Paola, B., and Bocchini, V. (1999) *Biochemistry 38*, 12288−12295.
19. Raimo, G., Masullo, M., Lombardo, B., and Bocchini, V. (2000) *Eur. J. Biochem. 267*, 6012−6017.
20. Masullo, M., Raimo, G., Parente A., Gambacorta, A., De Rosa, A., and Bocchini, B. (1991) *Eur. J. Biochem. 199*, 529−537.
21. Raimo, G., Masullo, M., Savino, G., Scarano, G., Ianniciello, G., Parente, A., and Bocchini, V. (1996) *Biochim. Biophys. Acta 1293*, 106−112.
22. Jones, T. A., Zou, J. Y., Cowan, S. W., and Kjeldgaard, M. (1991) *Acta Crystallogr. A47*, 110−119.
23. Kraulis, P. J. (1991) *J. Appl. Crystallogr. 24*, 946−950.
24. Merritt, E. A., and Bacon, D. J. (1997) *Methods Enzymol. 277*, 505−524.
25. Nyborg, J. (1998) *Acta Biochim. Pol. 45*, 883−894.
26. Nock, S., Grillenbeck, N., Ahmadian, M. R., Ribeiro, S., Kreutzer, R., and Sprinzl, M. (1995) *Eur. J. Biochem. 234*, 132−139.
27. Nissen, P., Kjeldgaard, M., Thirup, S., Polekhina, G., Reshetnikova, L., Clark, B. F., and Nyborg, J. (1995) *Science 270*, 1464−1472.
28. Nissen, P., Thirup, S., Kjeldgaard, M., and Nyborg, J. (1999) *Struct. Folding Des. 7*, 143−156.
29. Cammarano, P., Teichner, A., Chinali, G., Londei, P., De Rosa, M., Gambacorta, A., and Nicolaus, B. (1982) *FEBS Lett. 148*, 255−259.
30. Cammarano, P., Teichner, A., Londei, P., Acca, M., Nicolaus, B., Sanz, J. L., and Amilis, R. (1985) *EMBO J. 4*, 811−816.
31. Abdulkarim, F., Liljas, L., and Hughes, D. (1994) *FEBS Lett. 352*, 118−122.
32. Mesters, J. R., Zeef, L. A. H., Hilgenfeld, R., de Graaf, J. M., Kraal, B., and Bosch, L. (1994) *EMBO J. 13*, 4877−4855.
33. Vogeley, L., Palm, G. J., Mesters, J. R., and Hilgenfeld, R. (2001) *J. Biol. Chem. 276*, 17149−17155.

BI026428N